Excitonic and electron-hole processes in NaCl and NaCl:Ag crystals under conditions of multiplication of electronic excitations

2000 J. Phys.: Condens. Matter 12 1991

(http://iopscience.iop.org/0953-8984/12/9/304)

J. Phys.: Condens. Matter **12** (2000) 1991–2005. Printed in the UK PII: S0953-8984(00)05191-2

Excitonic and electron–hole processes in NaCl and NaCl:Ag crystals under conditions of multiplication of electronic excitations

E Feldbach†, M Kirm‡, A Lushchik†, Ch Lushchik† and I Martinson§

† Institute of Physics, University of Tartu, Riia 142, 51014 Tartu, Estonia
‡ II. Institute of Experimental Physics, University of Hamburg, Luruper Chaussee 149, D-22761 Hamburg, Germany
§ Department of Physics, Lund University, Sölvegatan 14, S-22362 Lund, Sweden

Received 15 June 1999, in final form 7 December 1999

Abstract. The excitation spectra of π and σ emissions of self-trapped excitons (3.4 eV and 5.4 eV, respectively) as well as the excitation spectra of 5.17 eV luminescence of Ag^+ impurity centres were measured in NaCl and NaCl:Ag crystals using synchrotron radiation of 5–38 eV. Fast and slow components of these emissions were detected. An analysis of the differences in the excitation spectra measured at 8 and 295 K allowed us to separate the excitonic and electron–hole (e–h) mechanisms of the multiplication of electronic excitations. A photon of 17–19 eV forms an e–h pair and a secondary exciton, while the absorption of a 21–27 eV photon causes the creation of two e–h pairs. Using luminescent and photoelectric methods, it was shown that a 2p3s Na^+ cation exciton, formed at the absorption of a 33.4 eV photon, decays with the creation of an anion exciton with a 3p hole component and two e–h pairs. Three e–h pairs are formed after the absorption of a 31 eV photon by a chlorine ion.

1. Introduction

Irradiation of wide-gap alkali halide crystals (AHCs) by vacuum ultraviolet (VUV) radiation in the region of fundamental absorption provides the creation of conduction electrons and free and self-trapped holes as well as of free and self-trapped excitons (see, e.g., [1]). In previous years, the excitonic and electron–hole (e–h) processes, that cause the excitation of the intrinsic luminescence of NaCl as well as the Tl^+ and Ag^+ impurity luminescence of doped NaCl crystals, have been investigated in detail under crystal irradiation by x-rays or photons of $h\nu \leqslant 11$ eV [2–4]. The use of synchrotron radiation (SR) allowed us to study the intrinsic and impurity luminescence in the case of NaCl excitation, when one absorbed photon is able to create two intrinsic electronic excitations (EEs), i.e. in the region of multiplication of electronic excitations (MEEs) [5–8]. Photoelectric investigations of NaCl have also been carried out (see, e.g., [9, 10]). It was shown that similarly to many other AHCs, the MEE process in NaCl involves the creation of secondary e–h pairs or secondary excitons by sufficiently 'hot' photoelectrons (HPEs) formed at the absorption of exciting photons [11–14]. The HPEs, the energy of which is smaller than the value of the energy gap E_g or even the formation energy of anion excitons, can provide a direct excitation of some luminescent impurity ions [15]. According to theoretical calculations [16–19] and experimental data on fundamental absorption [20–22] and the photoelectric effect [20, 23, 24], the photons of $h\nu > 32$ eV generate cation

0953-8984/00/091991+15$30.00

EEs in NaCl, while the threshold energy for electron transitions from the 3p and 3s states of chlorine ions to a conduction band is 8.8 [25] and more than 22 eV [26, 27], respectively.

The aim of the present study was to investigate in detail the excitonic and e–h processes in NaCl and NaCl:Ag crystals under conditions of MEEs. Recently, the creation processes of secondary excitons and secondary e–h pairs have been reliably separated in KBr and KI crystals at 8 K [11, 14, 28]. However, the existent data on the MEE processes in NaCl [5–8] were insufficient for a strict quantitative separation of the excitonic and e–h mechanisms of MEEs in the spectral region of 17–40 eV. We paid special attention to the investigation of the decay processes of cation excitons, formed due to $2p^6 \rightarrow 2p^5 3s$ transitions (33.4 eV) in Na^+.

2. Experimental details

Cubic face-centred NaCl crystals of high purity as well as crystals doped with Ag^+ impurity ions were the main objects of the present study. Single NaCl crystals were grown by the Stockbarger method from highly pure salt after an additional purification cycle involving a melt treatment in Cl_2 gas flow and a 50-fold recrystallization from the melt. Single NaCl:Ag crystals were grown by the Kyropoulos method in 'helium atmosphere'. The content of Ag^+ ions in a doped crystal was estimated by means of optical methods and is given in parentheses. The main experiments were carried out for NaCl:Ag (600 ppm), though NaCl:Ag (60 ppm) crystals were studied as well.

The main photoluminescence experiments were carried out at the SUPERLUMI station of HASYLAB at DESY, Hamburg. The experimental setup has been described in [29] and [30]. The excitation spectra were normalized to equal quantum intensities of SR falling onto the crystal. A typical spectral resolution of 0.3 nm (about 25 and 200 meV in the region of 10 and 30 eV, respectively) was used. The FWHM of SR pulses was 130 ps with a maximum repetition rate of 5 MHz. The excitation spectra were measured for time-integrated luminescence as well as for the emission detected within a time window (length Δt) correlated with the excitation pulses of SR (delayed by δt). Up to four time windows were set simultaneously. The delay δt and the length Δt were varied between 1 and 60 and 2 and 140 ns, respectively. Freshly cleaved samples were mounted in a cold-finger cryostat (8–300 K) and were studied under ultrahigh vacuum conditions ($\leqslant 10^{-9}$ mbar). Simultaneously with the excitation, the reflection spectra for the (100) plane of NaCl were recorded at an angle of incidence 17.5° from a sodium salicylate coated window by a XP2230B (Valvo) photomultiplier. The luminescence from a sample was analysed by a 0.5 m Czerny–Turner mounting monochromator equipped with a photomultiplier R2059 (Hamamatsu) operating in the time-correlated single photon counting mode. The emission spectra were not corrected on the spectral sensitivity of the detector and the transmittance of the monochromator. Some of the SR experiments were carried out at beamline 52 in the MAX-Laboratory in Lund, Sweden (550 MeV storage ring). Relevant details for the experimental setup have been described in a previous paper [11].

3. Experimental results

3.1. Luminescent manifestations of the MEE processes in NaCl at 8 K

The emission spectra of NaCl have been studied earlier in detail under a crystal photoexcitation in the region of fundamental absorption (see, e.g., [1, 2, 31, 32]). At $T = 5-10$ K, two emission bands with the maxima at 5.4 and 3.4 eV can be excited by photons of $h\nu > 9$ eV, that generate e–h pairs due to band-to-band transitions. These emission bands correspond to the radiative decay of singlet and triplet states of self-trapped excitons (STEs)—the so-called σ (5.4 eV) and π (3.4 eV) emissions.

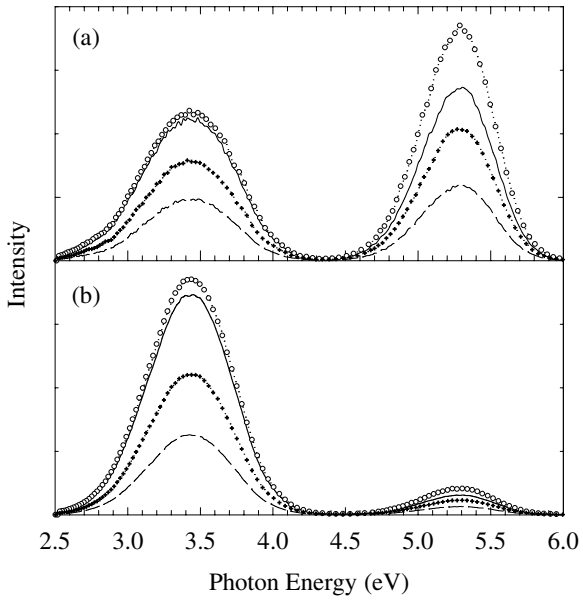

Figure 1. Luminescence spectra of NaCl in the case of excitation by photons of 19 eV (——), 25 (○), 31 (+) and 33.3 eV (– – –) at 8 K. The spectra are measured for time-integrated (b) and fast emissions (a) ($\Delta t = 12$ ns, $\delta t = 2.4$ ns).

Figure 1 shows the luminescence spectra measured for a time-integrated and a fast component ($\Delta t = 12$ ns and $\delta t = 2.4$ ns) in NaCl on excitation by photons of various energies (19, 25, 31 and 33.3 eV) at 8 K. According to our previous results [13], photons of 19 eV form holes in a valence band (v-band) and hot photoelectrons. These HPEs are able to create secondary anion excitons. Photons of $h\nu = 25$ eV produce HPEs able to generate secondary e–h pairs. Photons of 33.3 eV excite Na^+ ions up to $2p^5 3s$ state, i.e. create cation excitons [20, 22]. All four luminescence spectra contain π and σ emissions of STEs. The maximum for σ emission is slightly shifted with respect to its real position because of a decrease of the sensitivity of the emission registration channel in the spectral region above 5 eV. A π component dominates in all the time-integrated emission spectra, while σ emission is more intensive in a short time window. It is necessary to mention that the peak intensity ratio for π and σ emissions (both for time-integrated and fast emissions) in the case of excitation by 19 or 33.3 eV photons is about 20% higher than that at $h\nu = 25$ eV, when one absorbed photon provides the creation of two e–h pairs. It will be proved later that a photon of 19 and 33.3 eV forms an EE that undergoes a transformation into a secondary anion exciton and one or two e–h pairs. According to [32], π emission constitutes about 95% of a total STE emission in NaCl at the direct photogeneration of Γ excitons with $n = 1$, while its contribution becomes lower than 50% at the creation of excitons with $n = 2$ or at the recombination of electrons with self-trapped holes (V_K centres). Similarly to KBr [11, 14], our results allow us to conclude (see figure 1) that 19 eV photons produce mainly secondary excitons with $n = 1$. The effective radius of such excitons is $r_{eff} = 0.35$ nm [25]. The value of r_{eff} should decrease after the self-trapping of these secondary excitons.

According to Raman scattering measurements [33], the lowest state of STEs corresponds to a close F–H pair (an F centre and a Cl_2^- molecule in a closest-neighbour anion site) and not to the so-called V_Ke model of STE (an electron in a field of a V_K centre). Using the EPR

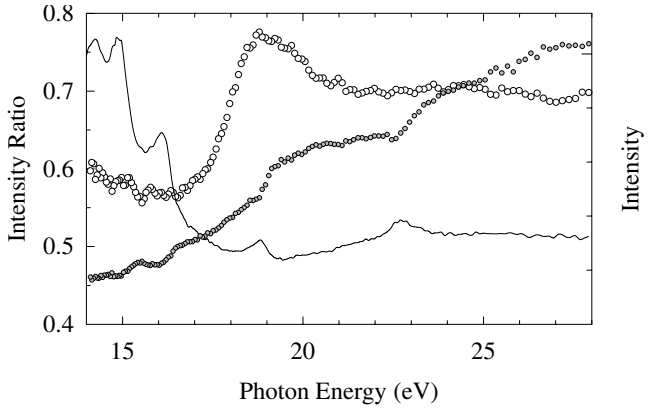

Figure 2. Reflection spectrum (——), excitation spectrum of time-integrated σ emission of STEs (●) and the intensity ratio spectrum (○) for π (3.4 eV) and σ (5.4 eV) STE emissions in NaCl at 8 K. The spectral sensitivity of the emission registration channel was taken into account in order to obtain absolute values of the ratio.

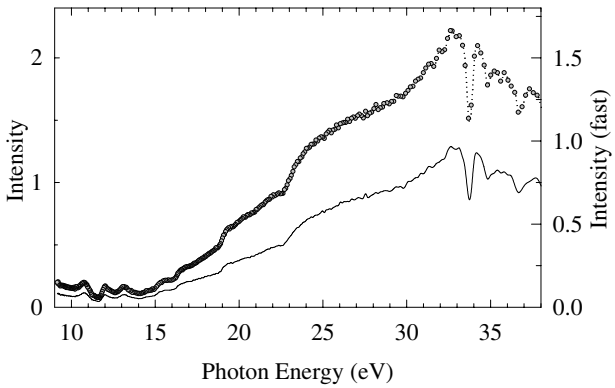

Figure 3. Excitation spectra for time-integrated (●) and fast component (——) of 5.5 eV emission of STEs ($\Delta t = 12$ ns, $\delta t = 2.4$ ns) in an NaCl crystal at 8 K.

method it was shown that, in contrast to KCl, KBr and KI crystals, a molecular axis of an H centre in NaCl is oriented along ⟨111⟩ directions [34]. In NaCl, the σ emission of STEs can be effectively excited at the recombination of electrons with V_K centres oriented along ⟨110⟩ similar to other AHCs.

Figure 2 presents the excitation spectrum of σ emission (5.4 eV) measured for NaCl in the region of 14–28 eV at 8 K. The intensity ratio spectrum for time-integrated π and σ emissions of STEs (I_π/I_σ) is depicted as well. The value of I_π/I_σ is practically constant in the region of 14 to 17 eV, it starts to increase at $h\nu \geqslant 17$ eV and reaches a maximum at 19 eV. Figure 3 shows the excitation spectrum for the time-integrated component of σ emission measured for another sample of NaCl in a wide spectral region of 9–38 eV at 8 K. A narrow dip at 33.4 eV corresponds to the creation of cation excitons. The efficiency of 5.5 eV emission η_σ is low in the region of 9–16 eV, i.e. at the interband electron transitions from the 3p Cl^- valence band to a complex conduction band formed by 3s Na^+, 3d Cl^- and 3d Na^+ states. In the region of 11–15 eV the value of intrinsic absorption reaches 5×10^6 cm^{-1} and a significant part of EEs non-radiatively annihilate in a thin near-surface layer. Fundamental absorption significantly

decreases if the photon energy exceeds the formation energy of longitudinal collective EEs—plasmons. In NaCl the plasmon formation energy is $E_{pl} = 15.5$ eV [35]. According to figure 3, the value of η_σ triples from 18 to 30 eV although the value of the absorption constant varies only slightly in this spectral region (see [21]). A further increase of η_σ takes place close to the formation region of cation EEs. A small dip is observed at 33.4 eV. According to [20] and [22], the excitation of Na^+ ions due to $2p^6 \rightarrow 2p^5 3s$ electron transitions, i.e. the creation of cation excitons takes place in the region of 33.4 eV.

Figure 3 presents also the excitation spectrum for the fast component ($\Delta t = 12$ ns and $\delta t = 2.4$ ns) of 5.5 eV emission. A peak intensity for a fast component is a factor of 2.5 lower than that for a time-integrated σ emission. The intensity of STE σ emission measured within a long window ($\Delta t = 137$ ns and $\delta t = 36$ ns) constitutes about 5% of a time-integrated signal and the excitation spectrum for this emission component is not presented in the figure.

3.2. Luminescent manifestations of the MEE processes in NaCl:Ag at 8 and 295 K

It is obvious that a strict separation of e–h and excitonic processes in the region of MEEs in NaCl can not be performed just on the basis of the results presented in [13] and section 3.1. Therefore, we carried out an additional detailed investigation of NaCl:Ag crystals, where besides STE emissions we had one more luminescent probe. Ag^+ ions isomorphically substitute Na^+ ions in regular lattice sites. The content of these impurity ions in NaCl can be smoothly increased up to high concentrations providing a variable ratio between single Ag^+ centres and Ag^+Ag^+ pairs. Single Ag^+ centres dominate in an NaCl:Ag (60 ppm) crystal, whereas up to 10% of the impurity ions exist as Ag^+Ag^+ pairs in NaCl:Ag (600 ppm). The luminescence of Ag^+ centres has been investigated in detail (see, e.g., [36] and references therein). At 8 K, the main emission band of Ag^+ centres is peaked at 5.17 eV (band-width $\delta = 0.15$ eV), while at room temperature the emission band broadens (the maximum at 5 eV). This emission mainly corresponds to $d^{10} \rightarrow d^9 s$ electron transitions in free Ag^+ ions. The long-wavelength excitation band of Ag^+ emission is peaked at 5.75 eV. The investigation of the excitation spectra for the recombination phosphorescence of Ag^+ centres ($T > 150$ K) led to the conclusion that the photoionization of these centres takes place at $h\nu \geqslant 6.4$ eV and the ground state of Ag^+ centres is located approximately 2.3 eV above the top of a v-band [37]. So, p holes in a v-band on NaCl:Ag can be effectively trapped by Ag^+ centres forming Ag^{2+} centres. The Ag^0 centres stable below 240 K are formed due to the trapping of electrons by Ag^+ centres. Both these centres, Ag^{2+} and Ag^0, are paramagnetic and have been investigated in detail by the EPR method (see [4] and references therein).

The spectrum of the recombination luminescence (RL) of Ag^+ centres coincides with that of the intracentre emission of Ag^+. The RL arises due to the recombination of conduction electrons (e) with Ag^{2+} centres via the intermediate excited state (*) of Ag^+ centres

$$Ag^+ + h + e \rightarrow Ag^{2+} + e \rightarrow (Ag^+)^* \rightarrow Ag^+ + h\nu_{Lum}. \tag{1}$$

In the case of high impurity concentration, the emission of Ag^+ centres arises also at the direct photocreation of mobile anion excitons (e^0) according to the following reaction:

$$Ag^+ + e^0 \rightarrow Ag^+e^0 \rightarrow (Ag^+)^* \rightarrow Ag^+ + h\nu_{Lum}. \tag{2}$$

The e–h and excitonic mechanisms of the excitation of Ag^+ centre luminescence have been studied earlier in a series of NaCl:Ag (the content of Ag^+ varies from 30 to 1000 ppm) in the temperature region of 80–400 K [4].

Different temperature dependences for e–h and excitonic mechanisms of Ag^+ emission excitation facilitate the separation of these mechanisms in the MEE region. The e–h mechanism is efficient only at a high mobility of holes. At $T < 160$ K, it is only the hot one-halide holes that

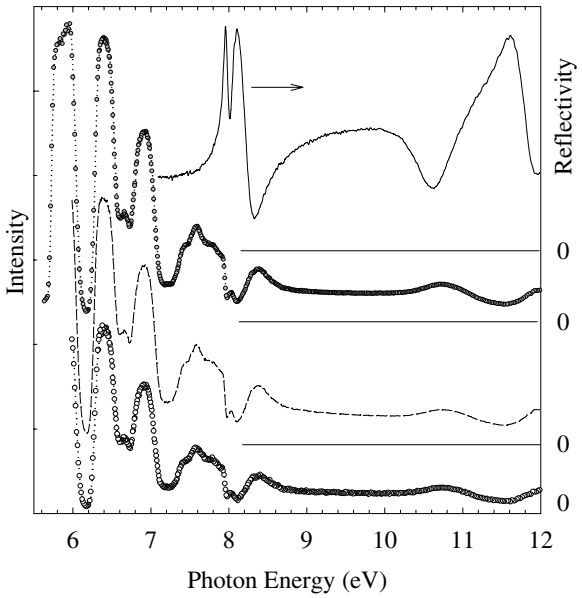

Figure 4. Reflection spectrum (——) and the excitation spectra for time-integrated (●), fast (Δt = 12.3 ns, δt = 1.7 ns) (○) and slow (Δt = 137 ns, δt = 36 ns) components (– – –) of 5.17 eV emission of Ag^+ centres in an NaCl:Ag (600 ppm) crystal at 8 K.

are mobile in NaCl, while the relaxed dihalide holes (V_K centres) are practically immobile. At $T > 160$ K, V_K centres participate in a hopping diffusion and interact with Ag^+ (the same as hot holes), forming Ag^{2+} centres and causing the appearance of RL. The cooling of NaCl:Ag (600 ppm) from 295 down to 8 K sharply freezes a part of the RL of Ag^+ centres. On the other hand, the excitonic mechanism of the energy transfer to Ag^+ centres is efficient at low temperatures. At higher temperatures, the mean free path of excitons before their transformation into STEs decreases. At $T > 100$ K, the main part of STEs in NaCl undergo non-radiative annihilation. So, the e–h mechanism of Ag^+ emission is dominant in NaCl:Ag at room temperature, while both the excitonic and e–h mechanisms are realized at 8 K.

Figure 4 presents the reflection spectrum and the excitation spectrum for time-integrated Ag^+ luminescence measured for NaCl:Ag (600 ppm) at 8 K. The 5.17 eV emission can be excited at the direct excitation of Ag^+ ions by 5.7–7.1 eV photons, while photons of $h\nu$ = 7.1–7.7 eV cause the excitation of the chlorine ions surrounding Ag^+ impurity ions. The Ag^+ emission can be excited also in the region of the exciton spin–orbital doublet (7.97 and 8.08 eV in the reflection spectrum). Taking into account selective reflection losses of SR, we can conclude that the efficiency of the excitonic mechanism of 5.17 eV emission excitation is about $\eta_{Ag} \approx 0.20$–0.25 in the region of 7.85 to 8.5 eV. In the spectral region of $h\nu$ = 8.8–12 eV, the value of η_{Ag} can be estimated as 0.13.

The intrinsic luminescence of STEs dominates in the emission spectrum of NaCl:Ag (60 ppm) for a crystal excitation in the long-wavelength region of a fundamental absorption (7.85 to 11 eV) at 8 K. A different situation arises for a NaCl:Ag (600 ppm) crystal. A narrow intense emission band of Ag^+ centres partly overlaps a broad-band σ emission of STEs (maximum at 5.4 eV). In order to separate the Ag^+ and σ emissions clearly, we measured the excitation spectrum for the 5.17 eV emission detected within a long time window (Δt = 137 ns and δt = 36 ns), when a fast σ emission is significantly decreased (see figure 4).

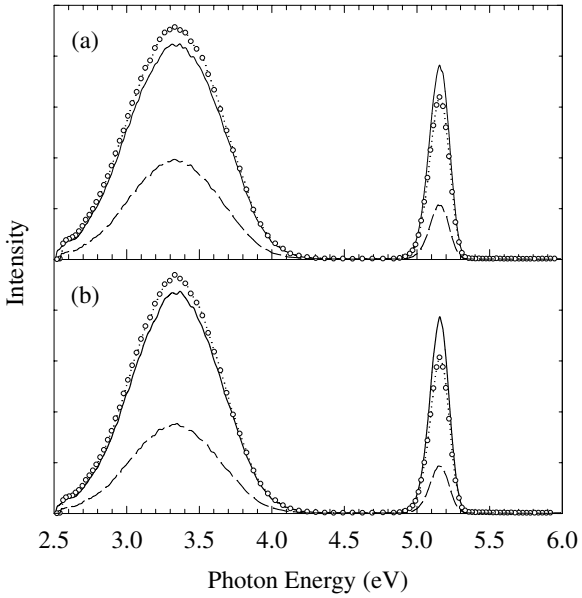

Figure 5. Luminescence spectra of NaCl:Ag (600 ppm) in the case of excitation by photons of 19 eV (——), 25 (○) and 33.3 eV (– – –) at 8 K. The spectra are measured for time-integrated (b) and slow emissions (a) ($\Delta t = 137$ ns, $\delta t = 36$ ns).

Figure 5 shows the time-integrated luminescence spectra measured for NaCl:Ag (600 ppm) at 8 K. The two main emission bands, the intrinsic π STE emission (3.35 eV) and the Ag^+ luminescence (5.17 eV), are observed in the case of a crystal excitation by 16 eV photons, i.e. below the threshold energy for the MEE process. The intensity ratio for these emissions I_{Ag}/I_π is the same at $h\nu = 25$ eV, when one absorbed photon is able to form two e–h pairs. However, the value of I_{Ag}/I_π is significantly higher in the case of NaCl:Ag excitation by 19 eV photons. For all the energies of exciting photons more than 60% of time-integrated 5.17 and 3.35 eV emissions are concentrated within a long window ($\Delta t = 137$ ns and $\delta t = 36$ ns).

Figure 6 presents the excitation spectrum for a time-integrated emission of Ag^+ centres measured in a wide spectral region for a NaCl:Ag (600 ppm) crystal at 8 K. The efficiency of impurity emission is low ($\eta_{Ag} \approx 0.10$–0.15) in the region of the intense bands of fundamental absorption (10 to 16 eV), the value of η_{Ag} sharply increases at 17–32 eV and then slightly decreases in the region of cation EE formation. The value of η_{Ag} at 32 eV is 1.4 times as high as that at the direct excitation of Ag^+ centres by 5.75 eV photons. Figure 6 depicts also the intensity ratio spectrum (I_{Ag}/I_σ) for the 5.17 eV emission of Ag^+ centres in NaCl:Ag and the σ emission of STEs (5.5 eV) in NaCl. The spectrum has a well marked maximum at 18.7 eV, a second, weaker maximum at 30 eV and several sharp peaks in the region of the fundamental absorption bands connected with the formation of cation EEs. The values of I_{Ag}/I_σ are equal at 16 and 25 eV, i.e. below and above the threshold energy for the formation of secondary e–h pairs. The maximum at 18.7 eV corresponds to the formation of both an e–h pair and a secondary anion exciton at the absorption of one exciting photon. The peak of I_{Ag}/I_σ at 33–34 eV coincides with the formation energy of cation excitons. It was mentioned earlier that the efficiency of the excitonic mechanism of Ag^+ luminescence excitation at 8 K is twice as high as that for the e–h mechanism (see figure 4). So, the behaviour of I_{Ag}/I_σ testifies that, in addition to e–h pairs, secondary anion excitons are created in the spectral regions of 17–20

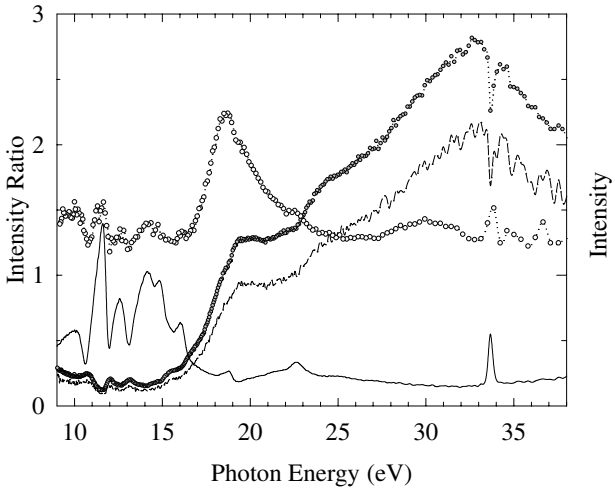

Figure 6. Reflection spectrum (——) and the excitation spectra for time-integrated 5.17 eV emission of Ag^+ centres (●) and for a fast emission of 5.17 eV (– – –) measured within a short time window ($\Delta t = 12$ ns, $\delta t = 2.4$ ns) in an NaCl:Ag (600 ppm) crystal at 8 K. The intensity ratio spectrum (○) for Ag^+ emission in NaCl:Ag and σ STE emission in NaCl at 8 K. The ratio is taken for time-integrated signals. The ordinate for the curve for a fast emission of 5.17 eV is multiplied by a factor of 25.

and 33–34 eV. A broad maximum of I_{Ag}/I_σ at 30 eV is connected also with the creation of secondary anion excitons. An energy of about 20–21 eV is needed to excite the $2s^2$ shell of Cl^- in NaCl [26]. Therefore, photons of 28–32 eV should form hot conduction electrons, the energy of which is sufficient for the creation of secondary anion excitons.

A comparative analysis of the data in figures 5 and 6 shows that the value of I_{Ag}/I_σ ratio for time-integrated signals at the excitation of an NaCl:Ag (600 ppm) crystal by 19 eV photons at 8 K is 2.3 times as high as that of I_{Ag}/I_π. This results is logical because the efficiency of Ag^+ centre emission as well as of the π emission of STEs is especially high in the creation region of secondary excitons with $n = 1$, while the σ emission of STEs is efficiently excited at the recombination of electrons and holes (compare with the case of KBr and KI crystals [14]). The analysis of the spectrum of I_{Ag}/I_σ was especially useful for the separation of the excitonic and e–h mechanisms of MEEs.

Figure 6 presents the excitation spectrum for the time-integrated 5.17 eV emission of Ag^+ centres as well as for the 5.17 eV emission measured within a short time window ($\Delta t = 12$ ns and $\delta t = 2.4$ ns) in NaCl:Ag (600 ppm). The intensity of the fast component is about 1/25 of that for the time-integrated emission of Ag^+ centres. A fast signal at 5.17 eV is partly connected with the tail of a broad-band σ emission of STEs with the maximum at 5.4 eV. The fast σ emission is notably intensive in a pure NaCl crystal, while it is weakened in NaCl:Ag (600 ppm). The presence of a large number of Ag^+ impurity ions, that serve as electron traps at 8 K, leads to a sharp decrease in the intensity of the σ recombination emission in NaCl:Ag.

Figure 7 shows the excitation spectrum of the 5 eV emission of Ag^+ centres measured for NaCl:Ag (600 ppm) at room temperature. At 295 K, the excitonic mechanism of Ag^+ emission excitation is suppressed, while the e–h mechanism is efficient due to the high mobility of V_K centres. So, the 5 eV emission is almost entirely caused by the e–h mechanism of the energy transfer to Ag^+ centres in a wide region of exciting photon energy (8.5 to 38 eV). Approximately one third of the e–h pairs, created by 9–16 eV photons in the region of strong interband absorption, undergoes a non-radiative recombination at the surface of a crystal. About 60% of

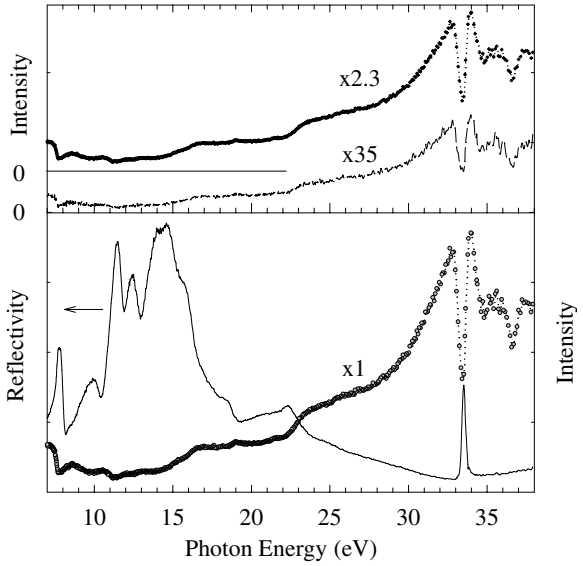

Figure 7. Reflection spectrum (——) and the excitation spectra for time-integrated (●), fast ($\Delta t = 9.7$ ns and $\delta t = 2.3$ ns) (– – –) and slow ($\Delta t = 130$ ns, $\delta t = 30$ ns) components (○) of 5 eV emission of Ag^+ centres in an NaCl:Ag (600 ppm) crystal at 295 K. The multiplication factor indicates the relative intensity for emissions measured within various time windows at the energy of exciting photons of 32 eV.

e–h pairs, formed by 17–21 eV photons (weak interband absorption), participate in the energy transport to Ag^+ centres in NaCl:Ag (600 ppm). At 295 K, the value of η_{Ag} does not increase at the efficient creation of secondary excitons by 17–21 eV photons. The efficiency of the e–h mechanism of Ag^+ emission starts to increase only at 21 eV and an especially sharp increase of η_{Ag} takes place at $h\nu > 22.5$ eV. The value of η_{Ag} doubles at 28 eV (with respect to its value at 22 eV) and even exceeds η_{Ag} at the direct excitation of Ag^+ centres by 5.8 eV photons. The value of η_{Ag} at 32 eV is more than twice that at the direct excitation of Ag^+ centres. However, there is a deep dip in the spectrum of η_{Ag} in the region of the direct creation of cation excitons (33–34 eV), where the value of η_{Ag} decreases down to the level of $h\nu = 28$ eV.

Figure 7 presents also the excitation spectra for the fast ($\Delta t = 9.7$ ns and $\delta t = 2.3$ ns) and slow components ($\Delta t = 130$ ns and $\delta t = 30$ ns) of Ag^+ centre emission measured in NaCl:Ag (600 ppm) at 295 K. The intensity of the fast and slow components is approximately 1/35 and half that for time-integrated emission, respectively. According to figure 7, the excitation spectra for the time-integrated, fast and slow components of 5 eV emission are slightly different only in the region of cation EEs ($h\nu > 34$ eV). A quantitative analysis of the data presented in figures 6 and 7 allows us to conclude that the e–h mechanism of Ag^+ emission excitation is dominant in NaCl:Ag (600 ppm) at 295 K, while, in addition, the excitonic mechanism becomes efficient and even dominates at 8 K.

4. Discussion of experimental results

4.1. Comparison of luminescent and photoelectric manifestations of MEEs with the band structure of NaCl

The band structure of NaCl has been calculated by several methods (see [16–19] and references therein). The calculations in the Hartree–Fock approximation with a subsequent inclusion of

correlation effects (mainly polarization ones) give the location of the minimum of the lowest 3s Na^+ conduction band (c-band) at the Γ point of the Brillouin zone. The maximum of the 3p Cl^- valence band is also located at the Γ point. A 3d-like c-band (mixed states of Cl^- and Na^+) is located above the bottom of 3s Na^+.

A detailed comparison of the calculated subbands of the c-band and the photon energies that cause the population of the corresponding states has been performed on the basis of the measurements of the angle dependence of photoelectric emission from a (100) surface of a single NaCl crystal [23]. The energy gap of $E_g = 8.8$ eV corresponds to $\Gamma_{15} \rightarrow \Gamma_1$ electron transitions in NaCl, while photons of 12.8 and 14.4 eV cause, respectively, $X'_5 \rightarrow X_1$ and $X'_4 \rightarrow X_1$ electron transitions from the v-band to the states located 2.4 eV above the bottom of the c-band [23]. The conduction electrons formed due to $X'_5 \rightarrow X_3$ and $X'_4 \rightarrow X_3$ transitions have a kinetic energy of 3.2 eV. The kinetic energy of non-relaxed conduction electrons (with respect to the bottom of the c-band) generated at $\Gamma_{15} \rightarrow \Gamma'_{25}$ ($h_\nu = 17.2$ eV), $\Gamma_{15} \rightarrow \Gamma_{12}$ (18.7 eV) and $X'_5 \rightarrow X_5$ (22.4 eV) electron transitions is 8.2, 9.7 and 12 eV, respectively. Taking into account even the weak processes of electron–phonon scattering while analysing the above-mentioned photoelectric data and band calculations, we can conclude that photons of 17.2 eV do not cause a creation of secondary e–h pairs in NaCl.

According to the data of electron spectroscopy, $\Gamma_{15} \rightarrow \Gamma'_{25}$ electron transitions take place at the absorption of 17.2 eV photons in NaCl [23]. The energy released at the subsequent $\Gamma'_{25} \rightarrow \Gamma_1$ Auger transition ($\approx$8.2 eV) is sufficient for the creation of a secondary Γ anion exciton with $n = 1$. $X'_5 \rightarrow X_4$ and $X'_4 \rightarrow X_4$ transitions (18.6 and 19.6 eV, respectively) produce HPEs with an energy of 8.2 eV above the bottom of the c-band as well [23]. According to figures 2 and 6, the intensity ratio I_π / I_σ in a pure NaCl crystal and I_{Ag} / I_σ in NaCl:Ag has a typical maximum at 17–19 eV connected with the creation of secondary free excitons with $n = 1$. These free excitons participate in the excitation of Ag^+ centre emission or undergo transformation into STEs and provide the appearance of π emission.

The typical peculiarities at 18.7 and 22.6 eV are observed in the reflection spectrum of NaCl (figure 6). These peculiarities are connected with $\Gamma_{15} \rightarrow \Gamma_{12}$ and $X'_5 \rightarrow X_5$ electron transitions [23]. The energy released at the subsequent $\Gamma_{12} \rightarrow \Gamma_1$ or $X_5 \rightarrow X_3$ Auger transition (9.8 and 9 eV, respectively) is sufficient for the creation of a secondary e–h pair. A decrease of the values of I_π / I_σ and I_{Ag} / I_σ in the region of 20–23 eV (figures 2 and 6) reflects the beginning of the creation of secondary e–h pairs by HPEs.

It was mentioned in section 3.2 that the e–h excitation mechanism of Ag^+ recombination luminescence dominates in NaCl at 295 K. According to figure 7, the value of η_{Ag} is practically constant in the region of 17–20 eV and sharply increases at $h\nu > 20$ eV due to the creation of secondary e–h pairs. The value of the photoelectric yield of NaCl sharply decreases at $h\nu = 17$–19 eV, i.e. when the creation of secondary excitons takes place, and the photoemission efficiency starts to increase at $h\nu > 20$ eV [9]. The value of electron affinity in NaCl is $\chi \approx 0.5$ eV [27]. So, the threshold energy of photons enabling creation of secondary e–h pairs does not exceed 20 eV.

The number of slow electrons in the energy distribution curve (EDC) of the emitted electrons in NaCl starts to increase with a rise of the exciting photon energy at $h\nu > 19.4$ eV due to the inelastic scattering of HPEs resulting in the creation of secondary e–h pairs [10]. At $h\nu = 21.2$ eV, slow (with a low E_{kin}) electrons dominate in the EDC of emitted electrons [38], as is natural for the region of 19.4–21.2 eV, where one absorbed photon causes the creation of two e–h pairs. The creation of stable F centres by VUV radiation has been studied in NaCl:Tl by means of luminescent methods [39]. It was shown that the efficiency of the F centre creation by 21.8 eV photons is 2.8 times as high as by 10 to 16.7 eV photons.

The threshold energy of exciting photons of $h\nu_t(\Gamma) = 2(E_g + \chi)$ is needed to create two e–h pairs (at the Γ point of the Brillouin zone) with hot electrons that are able to leave a crystal. In NaCl, $E_g = 8.8$ eV, $\chi \cong 0.5$ eV and $h\nu_t(\Gamma) = 18.6$ eV. If a similar process is connected with the electron transitions at the X point, then $h\nu_t(\mathrm{X}) > h\nu_t(\Gamma)$ because a part of the absorbed photon energy is gained by a hot photohole. According to the experimental data [23], a hole gains an energy of 1.4 or 2.6 eV at the electron transitions starting at X_5' and X_4' point in the v-band of NaCl, respectively. The threshold energies for such transitions are $h\nu_t(\mathrm{X}_5') = 20$ eV and $h\nu_t(\mathrm{X}_4') = 21.2$ eV. The energy of $\mathrm{X}_5' \rightarrow \mathrm{X}_4'$ transitions in NaCl equals 21 eV [23]. According to the data presented earlier, photons of 21 eV create secondary e–h pairs with hot holes, that provide the ionization of Ag^+ centres at the appearance of RL of Ag^+ centres in NaCl:Ag at 8 K.

4.2. Decay of cation excitons in NaCl

Manifestations of the creation of cation EEs have been detected at 30–40 eV in the absorption spectrum of NaCl at 295 K: a weak narrow A band (33.2 eV), a narrow intense B band (33.45 eV), a weak non-elementary C band (34.3–35.5 eV) and an intense D band (36.6 eV) [22]. Cooling of a crystal from 295 to 80 K causes a position shift of the most intense B band toward higher energies and the halving of the bandwidth (down to 150 meV). This B band is unambiguously interpreted as the creation of cation excitons due to the $2p^6 \rightarrow 2p^5 3s$ electron transitions in Na^+ ions. The temperature dependence of the width of the B band is proportional to $T^{1/2}$ that is typical of localized EEs. The position of the D absorption band shifts toward a low-energy region due to a crystal cooling. The D band is tentatively ascribed to $2p^6$ $Na^+ \rightarrow 2p^5 3d$ Na^+ electron transitions overlapping the continuum of band-to-band transitions [24].

An intense reflection peak at 33.5 eV in NaCl and NaCl:Ag (see figure 6) corresponds to the B absorption band of cation excitons at 8 K. At 295 K, the corresponding reflection peak in NaCl:Ag is situated at 33.4 eV (see figure 7). Deep dips at 33.4 and 36.5 eV in the excitation spectrum of Ag^+ centre emission (see figure 7) correlate with the B and D absorption bands of NaCl. Narrow peaks at 33.8 and 36.7 eV in the intensity ratio spectrum for Ag^+ luminescence and σ emission of STEs at 8 K (figure 6) are connected with the B and D absorption bands as well. The excitonic mechanism of Ag^+ centre excitation is dominant at 8 K. Therefore, the peak of I_{Ag}/I_σ at 33.8 eV (and probably at 36.7 eV), in our opinion, is (are) the manifestation of the creation of anion excitons due to the decay of cation excitons.

A deep dip in the region of 2p3s cation exciton creation (33.4 eV) is observed in the excitation spectrum of Ag^+ emission at 295 K (figure 7), when the e–h mechanism of impurity luminescence excitation is dominant. We interpret this dip as the decay of cation excitons into e–h pairs and anion excitons. At 295 K, anion excitons do not participate in the energy transfer to Ag^+ centres. A similar dip in the excitation spectrum of Ag^+ luminescence is detected in the region of the D absorption band (36.6 eV) as well. In free Na^+ ions the energy of $2p^6 \rightarrow 2p^5 3s$, $2p^6 \rightarrow 2p^5 3d$ and $2p^6 \rightarrow 2p^5 3p$ electron transitions equals 31.1, 36.9 and 41.1 eV, respectively, while the photoionization energy is 47.3 eV. So, the energy of $2p^6 \rightarrow 2p^5 3s$ transitions slightly differs for a free Na^+ ion and Na^+ ions in a crystal. However, the photoionization energy of Na^+ in a crystal is significantly lower than that in a free ion.

The decay of 2p3s Na^+ states was interpreted on the basis of interatomic Auger transitions resulting in the ionization of the states of neighbouring chlorine ions [22, 26]. Double Auger transitions can lead to the formation of two e–h pairs with hot electrons, that are able to create two more e–h pairs or two excitons. In NaCl at 10 K, $E_g = 8.8$ eV and the formation energy of anion excitons is $E_a = 8.0$ eV, while at 295 K the corresponding energies are $E_g \cong 8.6$ eV

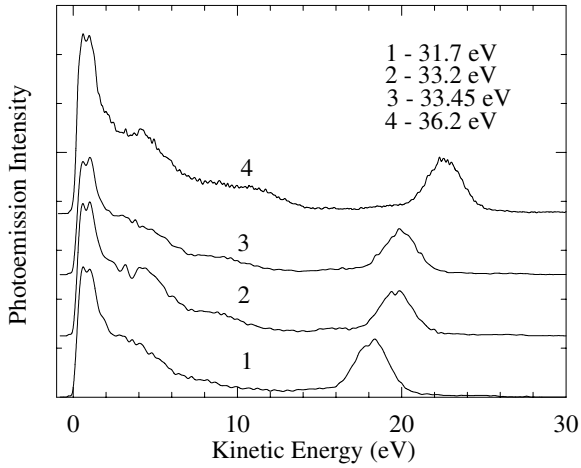

Figure 8. EDCs of an NaCl thin film for various exciting photon energies at 295 K.

and $E_a \cong 7.8$ eV [25]. So, the minimum energy needed for the creation of four e–h pairs or two e–h pairs plus two excitons at 10 K is 35.2 and 33.6 eV, respectively (34.4 and 32.8 eV at 295 K). However, it is necessary to take into account energy losses due to the vibronic relaxation of EEs, formed at the absorption of the exciting photons. Therefore, it is difficult to expect the formation of four EEs at the decay of a 2p3s cation exciton ($E_c = 33.7$ eV at 10 K and $E_c = 33.4$ eV at 295 K). In our opinion, one absorbed photon of 33.4 eV can provide the formation of three e–h pairs or two e–h and an exciton.

To choose between various possibilities of the cation exciton decay, available in terms of pure energetic conditions, we studied the energy distribution of the emitted electrons from a NaCl thin film excited by SR of 31 to 36 eV at 295 K. The photoelectron spectra were measured at beam-line 6A2 in the UVSOR facility in Okazaki, Japan (see [15] for experimental details). Figure 8 presents the measured EDCs. The energy of 31.7 eV is insufficient for the formation of cation EEs, while photons of 33.2 and 33.45 eV generate 2p3s cation excitons and 36.2 eV photons cause the ionization of $2p^6$ Na^+. All spectra are normalized to equal quantum intensities of SR falling onto the crystal by using the photoelectric yield of a gold mesh. The kinetic energy is given relative to a vacuum level.

According to figure 8, a significant part of the energy absorbed at the formation of cation excitons (for all four cases of excitation) is used for the creation of slow emitted electrons ($E_{kin} < 5$ eV), the energy of which is insufficient for the creation of secondary excitons or e–h pairs. This fact allows us to conclude that the decay of cation excitons provides the formation of three EEs (three e–h pairs or two e–h and an anion exciton) instead of four EEs as it was possible to suppose in terms of pure energetic considerations.

Our experimental results presented in section 3 testify to the decay of a 2p3s cation exciton with the creation of an anion exciton and two e–h pairs. At 295 K, excitons do not participate in the energy transfer to Ag^+ centres and the efficiency of Ag^+ emission sharply decreases in the region of 33.4 eV by 30% in NaCl:Ag (600 ppm) and by more than 50% in NaCl:Ag (60 ppm). On the other hand, the efficiency of Ag^+ recombination luminescence even increases 2.5 times due to crystal heating from 8 to 295 K in the case of excitation by 31.7 eV photons that provide the creation of three e–h pairs. In the latter case we have holes (V_K centres) highly mobile at 295 K. So, a narrow dip at 33–34 eV in the spectrum of η_{Ag} in NaCl:Ag (600 ppm) at 295 K reflects the presence of anion excitons formed at the absorption of 33.4 eV photons. According

to figure 7, the value of η_{Ag} at 33.4 eV is practically the same as at 28 eV, where one photon causes the formation of two e–h pairs (see section 4.1).

In a pure NaCl crystal at 8 K, an optically generated cation exciton can be transformed, due to several intermediate processes, into two e–h pairs and an anion exciton. This anion exciton undergoes self-trapping and a subsequent radiative decay with the appearance of π emission (3.38 eV), that can be easily detected in a slow time window or a time-integrated regime (see figure 1). σ emission of STEs (5.4 eV) is observed in a fast time window. There are only shallow dips at 33–34 eV in the excitation spectra for π and σ components of STE emission. The depth of these dips only slightly exceeds the reflection losses of SR in the region of the B absorption band ($\approx$7–8%). A fast component of the recombination σ emission in NaCl:Ag (600 ppm) at 8 K is weakened because of a partial prolonged localization of conduction electrons at Ag^+ centres as well as of the reabsorption of a broad-band σ emission by Ag^+ and Ag^+Ag^+ centres. At 8 K, Ag^+ luminescence is excited by non-relaxed anion excitons or at the recombination of electrons with Ag^{2+} centres formed with the participation of non-relaxed (hot) holes. The depth of the dip for η_{Ag} at 33.4 eV at 8 K is several times as small as that at 295 K, when excitons do not excite Ag^+ centres.

The selective absorption of localized cation EEs overlaps the continuum connected with the photoionization of the $3p^6$ and $3s^2$ shells of Cl^-. Therefore, the manifestations of the antiresonance of local and continuum states [40] can be expected in the region close to the intense B absorption band. The broad minimum at 30–32.5 eV is observed in the reflection (and consequently absorption) spectrum of NaCl:Ag (figure 7). Photons of 30–32.5 eV penetrate into a thick crystal layer causing the decrease of the yield of photoelectric emission (figure 8), weakening near-surface recombination and increasing the efficiency of the recombination luminescence of Ag^+ centres (figure 7). In agreement with the theory [40] the cooling of NaCl causes the transformation of the shape of the B absorption band (Gaussian $\rightarrow$ antisymmetric Lorentzian) [22].

The real sequence of elementary processes, resulting either in the decay of a cation exciton into an anion exciton with 3p hole component and two e–h pairs or in the creation of three e–h pairs due to the photoionization of Cl^-, is the most difficult question. The photoionization of the outer $3p^6$ Cl^- shell by a 36 eV photon causes the creation of a conduction electron, the energy of which is 8.8–12.8 eV lower than the energy of the exciting photon (in NaCl, a total width of the v-band is slightly less than 4 eV [19, 27] and $E_g = 8.8$ eV). According to figure 8, photons of 36.2 eV provide the appearance of the emitted electrons with the maximum energy of 24 eV, although the main part of electrons from this group has the energy of 22.5 eV. Inside thick crystals such HPEs can undoubtedly create the second e–h pair. A group of electrons with $E_{kin} = 9 - 13$ eV (see figure 8) is able to create the third e–h pair.

A group of the emitted electrons with the maximum energy of $E_{kin} = 22$ eV is observed in EDCs of an NaCl film at the excitation of Na^+ ions ($2p^6 \rightarrow 2p^5 3s$) by 33.2 or 33.45 eV photons (figure 8). However, the value of photoelectric yield at $h\nu = 33$–34 eV is 30% lower than that in the case of the exciting photons of $h\nu = 36.2$ eV. EDCs contain another group of electrons with $E_{kin} = 8$–9.5 eV, the energy of which is sufficient for the creation of secondary excitons, but is not enough to form secondary e–h pairs. So, the data obtained by luminescent and photoelectric methods allow us to conclude that the decay of a cation exciton in NaCl leads to the creation of an anion exciton and two e–h pairs. One of the possible decay mechanisms of cation excitons can be ascribed to the Auger process with the energy transfer from an excited outer shell of Na^+ to two neighbouring chlorine ions, one of which will be in an excited state, while another Cl^- will be ionized forming a high-energy conduction electron.

A similar hypothesis on the decay of cation excitons has been recently considered for a KBr crystal [28]. Significant differences in the creation processes of the groups of spatially

correlated defects at 8 K were observed in the case of cation exciton formation or at the photoionization of the $3p^6$ shell of K^+. It is obvious that a further comparative theoretical analysis of various mechanisms of cation exciton decay resulting in the creation of an anion exciton and two e–h pairs is needed.

5. Concluding remarks

A highly sensitive luminescent method for the separation of the creation processes of secondary excitons and electron–hole pairs in NaCl crystals has been elaborated. The analysis of the differences in the excitation spectra for intrinsic and impurity emissions in NaCl and NaCl:Ag allowed us to conclude that one photon of 17–20 eV leads to the formation of a hot p-hole and a hot conduction electron, and the energy of a hot photoelectron is sufficient to create a secondary anion exciton. Photons of $h\nu > 20$ eV provide the creation of secondary e–h pairs. The obtained experiment results are in a good agreement with the photoelectric data [9, 10, 23] and band structure calculations for NaCl [16, 17, 19]. The luminescent and photoelectric manifestations of the decay of a 2p3s cation exciton resulting in the creation of an anion exciton with a 3p-hole component and two e–h pairs are detected.

Acknowledgments

We are grateful to Professor G Zimmerer from the Hamburg University for valuable discussions and to Professor M Kamada from the Institute for Molecular Science, Okazaki for assistance in the photoelectric measurement. This work has been partly supported by the Estonian Science Foundation (grant 3868), the Crafoord Foundation and the STINT Foundation (Sweden) and the University Exchange Program between Hamburg and Tartu.

References

[1] Song K S and Williams R T 1993 *Self-Trapped Excitons* (Berlin: Springer)
[2] Kabler M N 1964 *Phys. Rev.* **136** A1296
[3] Lushchik Ch B, Liidja G G and Elango M A 1964 *Sov. Phys.–Solid State* **6** 1789
[4] Vasil'chenko E A, Lushchik N E and Lushchik Ch B 1970 *Sov. Phys.–Solid State* **12** 167
[5] Ivanov S N, Ilmas E R, Lushchik Ch B and Mikhailin V V 1973 *Sov. Phys.–Solid State* **15** 1053
[6] Onuki H and Onaka R 1973 *J. Phys. Soc. Japan* **34** 720
[7] Beamont J H, Bourdilon A J and Kabler M N 1976 *J. Phys. C: Solid State Phys.* **9** 2961
[8] Yanagihara M, Kondo Y and Kanzaki H 1983 *J. Phys. Soc. Japan* **52** 4397
[9] Duckett S W and Metzger P H 1965 *Phys. Rev.* **137** 953
[10] Onuki H 1974 *Sci. Light* **23** 54
[11] Lushchik A, Feldbach E, Lushchik Ch, Kirm M and Martinson I 1994 *Phys. Rev.* B **50** 6500
[12] Ejiri A, Hatano A and Nakagawa K 1994 *J. Phys. Soc. Japan* **63** 314
[13] Kirm M, Frorip A, Kink R, Lushchik A, Lushchik Ch and Martinson I 1995 *Radiat. Eff. Defects Solids* **135** 375
[14] Lushchik A, Feldbach E, Kink R, Lushchik Ch, Kirm M and Martinson I 1996 *Phys. Rev.* B **53** 5379
[15] Feldbach E, Kamada M, Kirm M, Lushchik A, Lushchik Ch and Martinson I 1997 *Phys. Rev.* B **56** 13 908
[16] Kunz A B and Lipari N O 1971 *Phys. Rev.* B **4** 1374
[17] Lipari N O and Kunz A B 1971 *Phys. Rev.* B **3** 491
[18] Pantelides S T 1975 *Phys. Rev.* B **6** 2391
[19] Kunz A B 1982 *Phys. Rev.* B **26** 2056
[20] Haensel R, Keitel G, Schreiber P and Sonntag B 1968 *Phys. Rev. Lett.* **20** 1436
[21] Roessler D M and Walker W C 1968 *Phys. Rev.* **166** 599
[22] Nakai S, Ishii T and Sagawa T 1971 *J. Phys. Soc. Japan* **30** 428
[23] Himpsel F and Steinmann W 1978 *Phys. Rev.* B **17** 2537
[24] Iwan M and Kunz C 1978 *J. Phys. C: Solid State Phys.* **11** 905

[25] Miyata T and Tomiki T 1968 *J. Phys. Soc. Japan* **24** 1286
[26] Elango M, Ausmees A, Kikas A, Nõmmiste E, Ruus R, Saar A, van Acker J F, Andersen J N, Nyholm R and Martinson I 1993 *Phys. Rev.* B **47** 11 736
[27] Poole R T, Jenkin J G, Liesegang J and Leckey C G 1975 *Phys. Rev.* B **11** 5179
[28] Kirm M, Lushchik A, Lushchik Ch, Martinson I, Nagirnyi V and Vasil'chenko E 1998 *J. Phys.: Condens. Matter* **10** 3509
[29] Zimmerer G 1991 *Nucl. Instrum. Methods Phys. Res.* A **308** 178
[30] Kirm M, Zimmerer G, Feldbach E, Lushchik A, Lushchik Ch and Savikhin F 1999 *Phys. Rev.* B **60** 502
[31] Pooley D and Runciman W A 1970 *J. Phys. C: Solid State Phys.* **3** 1815
[32] Matsumoto T, Kawata T, Miyamoto A and Kan'no K 1992 *J. Phys. Soc. Japan* **61** 4229
[33] Suzuki T, Tanimura K and Itoh N 1994 *Phys. Rev.* B **49** 7233
[34] Lushchik A Ch and Frorip A G 1990 *Phys. Status Solidi* b **161** 525
[35] Creuzburg M 1966 *Z. Phys.* **196** 433
[36] Niilisk A and Laisaar A 1969 *Phys. Status Solidi* **33** 851
[37] Kuketayev T, Lushchik N and Lushchik Ch 1972 *Trudy Inst. Fiz. Akad. Nauk Est. SSR* **39** 140
[38] Newburg G 1963 *Phys. Rev.* **132** 1570
[39] Ilmas E and Lushchik Ch 1966 *Izv. Akad. Nauk SSSR Ser. Fiz.* **30** 654
[40] Toyozawa Y, Inoue M, Inui T, Okazaki M and Hanamura E 1967 *J. Phys. Soc. Japan* **22** 1337